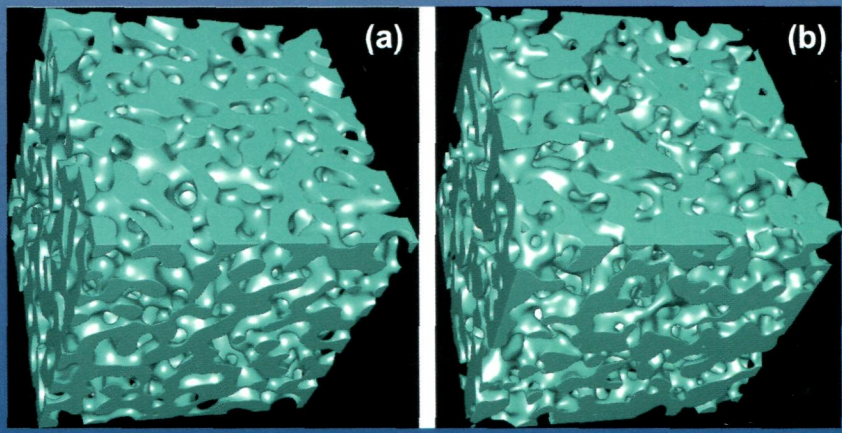
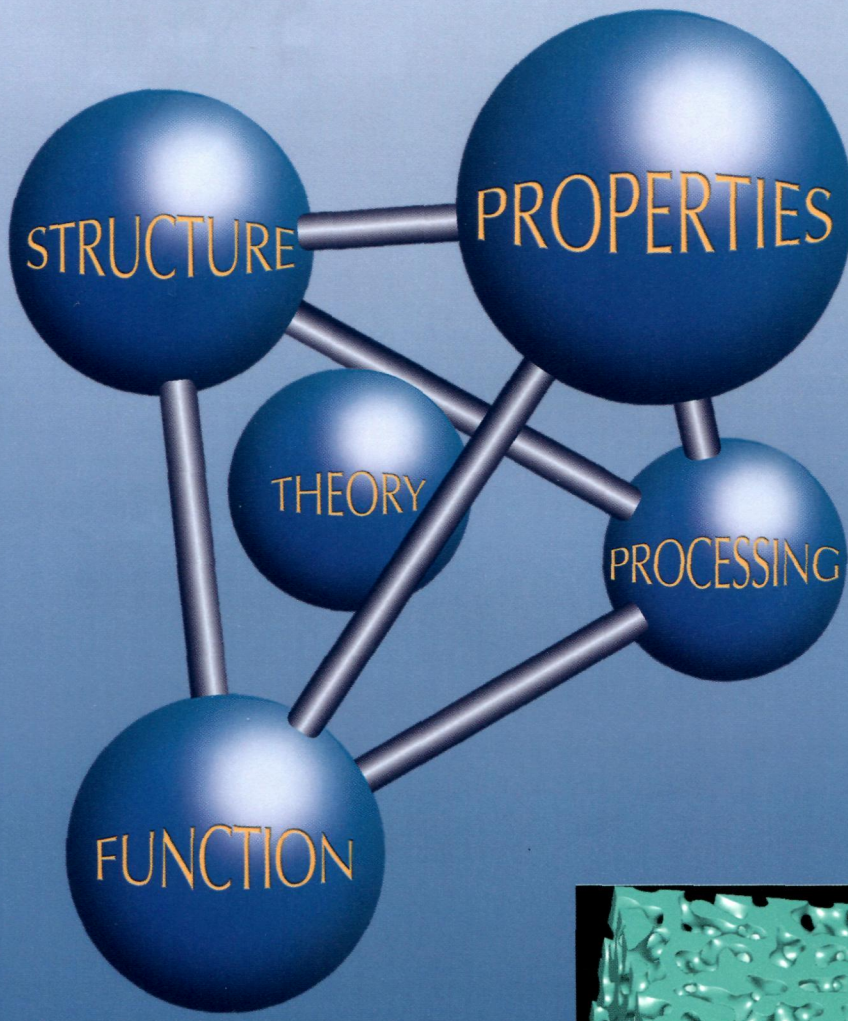


Volume 61, Issue 4, February 2013

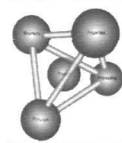
ISSN 1359-6454

Acta MATERIALIA





ELSEVIER



Acta MATERIALIA

www.elsevier.com/locate/actamat

Acta MATERIALIA

VOLUME 61

PUBLISHED 15 JANUARY 2013

ISSUE 4

v 2013 Acta Materialia Gold Medal Award

- A. Hosokawa, D. S. Wilkinson, J. Kang and E. Maire 1021 Onset of void coalescence in uniaxial tension studied by continuous X-ray tomography
- X. Zhang, M. Watanabe and S. Kuroda 1037 Effects of processing conditions on the mechanical properties and deformation behaviors of plasma-sprayed thermal barrier coatings: Evaluation of residual stresses and mechanical properties of thermal barrier coatings on the basis of in situ curvature measurement under a wide range of spray parameters
- E. R. Homer, S. M. Foiles, E. A. Holm and D. L. Olmsted 1048 Phenomenology of shear-coupled grain boundary motion in symmetric tilt and general grain boundaries
- P. Neumeister, M. Jurisch, H. Jelitto, A. R. Engert, G. A. Schneider and H. Balke 1061 Effective permittivity of air-filled cracks in piezoelectric ceramics due to crack bridging
- R. Bassiri, K. Evans, K. B. Borisenko, M. M. Fejer, J. Hough, I. MacLaren, I. W. Martin, R. K. Route and S. Rowan 1070 Correlations between the mechanical loss and atomic structure of amorphous TiO₂-doped Ta₂O₅ coatings
- E. Davidoff, P. K. Galenko, D. M. Herlach, M. Kolbe and N. Wanderka 1078 Spinodally decomposed patterns in rapidly quenched Co–Cu melts
- M. Z. Alam, S. V. Kamat, V. Jayaram and D. K. Das 1093 Tensile behavior of a free-standing Pt-aluminide (PtAl) bond coat
- A. Umantsev 1106 Nanophases of binary and multicomponent alloys
- Y. K. Chen-Wiegart, S. Wang, W.-K. Lee, I. McNulty, P. W. Voorhees and D. C. Dunand 1118 *In situ* imaging of dealloying during nanoporous gold formation by transmission X-ray microscopy
- M. Dragomir, I. Arčon, S. Gardonio and M. Valant 1126 Phase relations and optoelectronic characteristics in the NdVO₄–BiVO₄ system
- Q.-M. Hu and R. Yang 1136 Basal-plane stacking fault energy of hexagonal close-packed metals based on the Ising model
- I. Castro-Hurtado, C. Malagù, S. Morandi, N. Pérez, G. G. Mandayo and E. Castaño 1146 Properties of NiO sputtered thin films and modeling of their sensing mechanism under formaldehyde atmospheres

[continued on inside back cover]

Available online at www.sciencedirect.com**SciVerse ScienceDirect**

1359-6454(201302)61:4;1-0

Acta mater. is Indexed/Abstracted in: Appl. Mech. Rev.; Res. Alert; Chem. Abstr. Serv.; Curr. Cont./Phys. Chem. Earth Sci.; Curr. Cont./Engng Tech. Appl. Sci.; Ed. Metals Abstr.; Engng Ind.; IBZ & IBR; INSPEC Data.; Metals Abstr.; PASCAL-CNRS Data.; Curr. Cont. Sci. Cit. Ind.; Curr. Cont. SCISEARCH Data.; SSSA/CISA/ECA/ISMEC; MSCI; Also covered in the abstract and citation database SciVerse Scopus®. Full text available on SciVerse ScienceDirect®.

ISSN 1359-6454

[CONTENTS—continued from outside back cover]

- E. Jimenez-Melero, R. Blondé, M. Y. Sherif,
V. Honkimäki and N. H. van Dijk
- S. V. Zherebtsov, G. S. Dyakonov, A. A. Salem,
V. I. Sokolenko, G. A. Salishchev and
S. L. Semiatin
- H. Wang, B. Clausen, C. N. Tomé and P. D. Wu
- H. Song and J. J. Hoyt
- H. Mughrabi
- Y. Tong, W. Dmowski, Z. Witczak, C.-P. Chuang and
T. Egami
- T. Hu, J. H. Chen, J. Z. Liu, Z. R. Liu and C. L. Wu
- S. O. Poulsen, P. W. Voorhees and E. M. Lauridsen
- R. P. Shi, C. P. Wang, D. Wheeler, X. J. Liu and
Y. Wang
- S. Zabler, A. Ershov, A. Rack, F. Garcia-Moreno,
T. Baumbach and J. Banhart
- S. Romankov, Y. C. Park, I. V. Shchetinin and
J. M. Yoon
- A. Pakdel, X. Wang, Y. Bando and D. Golberg
- D.-K. Lim, H.-N. Im, S.-Y. Jeon, J.-Y. Park and
S.-J. Song
- F. X. Qin, N. S. Bingham, H. Wang, H. X. Peng,
J. F. Sun, V. Franco, S. C. Yu, H. Srikanth and
M. H. Phan
- Y. Onuki, R. Hongo, K. Okayasu and H. Fukutomi
- A. Bogno, H. Nguyen-Thi, G. Reinhart, B. Billia and
J. Baruchel
- E. J. Payton, G. Wang, M. J. Mills and Y. Wang
- S. Dai, Y. Xiang and D. J. Srolovitz
- H. Chen and S. van der Zwaag
- R. Dittmer, K. G. Webber, E. Aulbach, W. Jo,
X. Tan and J. Rödel
- K. Wang, H. Wang, F. Liu and H. Zhai
- 1154 Time-dependent synchrotron X-ray diffraction on the austenite decomposition kinetics in SAE 52100 bearing steel at elevated temperatures under tensile stress
- 1167 Formation of nanostructures in commercial-purity titanium via cryorolling
- 1179 Studying the effect of stress relaxation and creep on lattice strain evolution of stainless steel under tension
- 1189 An atomistic simulation study of the migration of an austenite–ferrite interface in pure Fe
- 1197 Cyclic slip irreversibility and fatigue life: A microstructure-based analysis
- 1204 Residual elastic strain induced by equal channel angular pressing on bulk metallic glasses
- 1210 The crystallographic and morphological evolution of the strengthening precipitates in Cu–Ni–Si alloys
- 1220 Three-dimensional simulations of microstructural evolution in polycrystalline dual-phase materials with constant volume fractions
- 1229 Formation mechanisms of self-organized core/shell and core/shell/corona microstructures in liquid droplets of immiscible alloys
- 1244 Particle and liquid motion in semi-solid aluminium alloys: A quantitative *in situ* microradioscopy study
- 1254 Atomic-scale intermixing, amorphization and microstructural development in a multicomponent system subjected to surface severe plastic deformation
- 1266 Nonwetting “white graphene” films
- 1274 Experimental evidence of hydrogen–oxygen decoupled diffusion into $\text{BaZr}_{0.6}\text{Ce}_{0.25}\text{Y}_{0.15}\text{O}_{3-\delta}$
- 1284 Mechanical and magnetocaloric properties of Gd-based amorphous microwires fabricated by melt-extraction
- 1294 Texture development in Fe–3.0 mass% Si during high-temperature deformation: Examination of the preferential dynamic grain growth mechanism
- 1303 Growth and interaction of dendritic equiaxed grains: *In situ* characterization by synchrotron X-ray radiography
- 1316 Effect of initial grain size on grain coarsening in the presence of an unstable population of pinning particles
- 1327 Structure and energy of (111) low-angle twist boundaries in Al, Cu and Ni
- 1338 Analysis of ferrite growth retardation induced by local Mn enrichment in austenite created by prior interface passages
- 1350 Electric-field-induced polarization and strain in $0.94(\text{Bi}_{1/2}\text{Na}_{1/2})\text{TiO}_3 - 0.06\text{BaTiO}_3$ under uniaxial stress
- 1359 Modeling rapid solidification of multi-component concentrated alloys

[CONTENTS—continued from inside back cover]

- M. R. Tonks, Y. Zhang, S. B. Biner, P. C. Millett and X. Bai 1373 Guidance to design grain boundary mobility experiments with molecular dynamics and phase-field modeling
- Q. S. Pan, Q. H. Lu and L. Lu 1383 Fatigue behavior of columnar-grained Cu with preferentially oriented nanoscale twins
- E. Bitzek and P. Gumbsch 1394 Mechanisms of dislocation multiplication at crack tips
- H. Beladi and G. S. Rohrer 1404 The relative grain boundary area and energy distributions in a ferritic steel determined from three-dimensional electron backscatter diffraction maps
- L. Cao and M. Koslowski 1413 Effect of microstructural uncertainty on the yield stress of nanocrystalline nickel